Partial least squares regression as a tool to predict fluoropolymer surface modification by dielectric barrier discharge in a corona process configuration in a nitrogen-organic gaseous precursor environment

LABORATOIRE LIS D'INGÉNIERIE DE SURFACE

Julien Vallade, Stéphane Turgeon, and Gaétan Laroche

Laboratoire d'Ingénierie de Surface (LIS), Département de Génie des Mines, de la Métallurgie et des Matériaux, Centre de Recherche sur les Matériaux Avancés (CERMA), Université Laval, Québec G1V 0A6, Canada
Hôpital St-François d'Assise, Centre de Recherche du Centre Hospitalier Universitaire de Québec (CRCHUQ), Québec G1L 3L5, Canada

ABSTRACT
A dielectric barrier discharge in a corona process configuration is used to treat the surface of fluoropolymers in a nitrogen/organic precursor environment. The surface chemistry, thickness, and water contact angle of the deposited coatings are measured and used to build up an output matrix to be correlated with an input matrix built using electrical parameters of the discharge, the gas mixture chemical composition, and spectroscopic parameters measured in both the infrared and UV-Vis emission spectral regions. Partial least square regression (PLSR) model enables determining the most important plasma parameters to drive the coating physicochemical characteristics. From the PLSR model, it turns out that the plasma electrical parameters drive the surface modification process, at the expense of other plasma characteristics such as gas flow, gaseous precursor concentration, nitrogen vibrational temperature, and the level of gaseous precursor conversion within the plasma.

KEYWORDS
Corona processes; dielectric barrier discharges; fluoropolymers; surface modifications; partial least square regression; plasma characterization; surface characterization

CITATION
Vallade, J., Turgeon, S., & Laroche, G. (2018). Partial Least-Squares Regression as a Tool To Predict Fluoropolymer Surface Modification by Dielectric Barrier Discharge in a Corona Process Configuration in a Nitrogen–Organic Gaseous Precursor Environment. Industrial & Engineering Chemistry Research, 57(22), 7476-7485.

This is the author's version of the original manuscript. The final publication is available at ACS Link Online via DOI: 10.1021/acs.iecr.8b00228

1 INTRODUCTION

Fluoropolymers are industrial raw materials used in many economic sectors such as automotive, textile, building, energy, and biomedical.[1,2] If the chemical inertness and anti-adhesive properties which characterize these materials are the cause of their success, these remarkable qualities turn

into a major flaw for applications where they need to be glued to other materials. Indeed, modifying their surface properties becomes a mandatory step prior to any use. Different solutions to solve this problem have been proposed in the literature. Among the latter, the redox treatment, which generally results in the formation of polymeric carbon, is the most used.[3,4] One way to provide the reduction of C-F bonds is the use of plasma treatments that are well-known as an environmentally friendly technology due to the low reactive quantity used to treat large sample areas. Historically, low pressure plasmas were used for surface modifications of polymers. However, recent researches have shown the possibility to modify the surface or to perform thin films deposition using Dielectric Barrier Discharges (DBD) on various fluorinated polymers.[5] Atmospheric DBD plasmas are advantageous surface modification technologies from an industrial point of view because they do not require to use vacuum systems that prolong the treatment time and require extended maintenance.

In the present study, mixtures of nitrogen and an organic gaseous precursor were used to treat three different fluoropolymers, namely fluorinated ethylene polypropylene (FEP), polytetrafluoroethylene (PTFE), and ethylene tetrafluoroethylene (ETFE). As the aim of the surface modification was to improve the wettability of these polymers, the reactive gas mixed with nitrogen was carefully chosen to create a gas environment to bring various kinds of hydrophilic functional groups at the surface such as OH, NH_x or COOH to hopefully improve the adhesion properties.

More than just showing the possibility to modify the surface properties of fluorinated polymers, the aim of the present study was to identify the plasma parameters that are of importance to control the surface chemistry of the plasma-deposited films. For instance, several plasma parameters such as gas flow or gas concentration, power density, waveform of excitation, frequency of the signal, etc., need to be tuned to get surfaces with appropriate surface characteristics. All of these plasma parameters may influence the chemistry of the deposited layer and accordingly, have been the subject of many investigations in previous studies.[6-11] Basically, these researches were based on extensive studies requiring several experiments where each of the plasma parameters of interest were modified independently while trying to correlate their influence with the coating surface chemistry using analytical techniques such as x-ray photoelectron spectroscopy (XPS), Fourier Transform infrared spectroscopy (FTIR), or time-of-flight secondary ion mass spectroscopy (TOF-SIMS).[12-17] Despite having brought a lot of information, such an approach is time consuming and often leads to results that are difficult to interpret or simply contradictory.[18,19] In this context, Partial Least Squares Regression (PLSR) was identified as a tool that allows to unambiguously evidence relationships between plasma experimental parameters and surface coatings chemistry. Basically, PLSR modelling correlates two matrices;[20] the first one, the input matrix, being filled with plasma parameters while the surface properties are used to construct the output matrix. Such a study has already been successfully used to characterize the effect of the experimental characteristics of a microwave low pressure plasma in a nitrogen-hydrogen environment on PTFE surfaces.[21] That research showed that emission spectroscopy recorded from the light emitted by plasmas can be used to predict the resulting treated polymer surface chemistry. This means that, in addition to a better understanding of the plasma process, PLSR modelling can be used to predict the surface properties of plasma modified/coated surfaces as a function of plasma parameters. Such a process control is of paramount importance in industrial processes since it allows avoiding the expensive and time-consuming post-plasma surface characterization.

Accordingly, the surface chemistry, thickness, and water contact angle of the deposited coatings were measured and used to build up an output matrix to be correlated with an input matrix built using electrical parameters of the discharge, the gas mixture chemical composition, and spectroscopic parameters measured in both the infrared and UV-Vis emission spectral regions. The PLSR models allowed determining the most important plasma parameters to control the coating physicochemical characteristics, thanks to the calculation of the variable importance on the projection (VIP). The PLSR loading biplots also helped to interpret the relationships between the plasma parameters and surface properties.

2 EXPERIMENTAL SECTION

2.1 Plasma reactor

Figure 1 is a schematic illustration of this discharge cell. The discharge cell was made of two electrically connected bars of stainless steel, which constitute the powered electrodes. The bar surfaces were 300 mm x 15 mm and were connected on the audio frequency high voltage provided by the power supply. The gas was injected between the two bars through a slit of 1.5 mm over the whole length of the 300 mm-long electrodes. It flowed in the two plasma zones located between the grounded and the high voltage electrodes. The grounded electrode was a stainless-steel cylinder of 150 mm diameter. The polymer films to be treated (150 µm thick) were put against the grounded electrode and acted as a dielectric barrier avoiding spark transition that would lead to the destruction of the polymers. The power supply was built from an AFG2021 arbitrary function generator from Tektronix, Inc. (Beaverton, OR, USA) plugged into a PL380 audio amplifier from QSC Audio Products, LLC (Costa Mesa, CA, USA) which can deliver up to 8 kW at 100 V_{pp}. The low voltage was converted to high voltage, thanks to a transformer manufactured by Raftabtronics (DeLand, FL, USA) that allowed reaching 28 kV_{pp} between 5 and 15 kHz. The discharge was generated in nitrogen at atmospheric pressure with a few percent of the gaseous precursor. The flows were controlled by gas and liquid (EL-Flow and Liqui-Flow) mass flow controllers with a Controlled Evaporator and Mixer (CEM) all from Bronkhorst High-Tech B.V. (Ruurko, Holland). Under these conditions, a filamentary dielectric barrier discharge was obtained, and the surface properties of the polymer films were thereby modified.

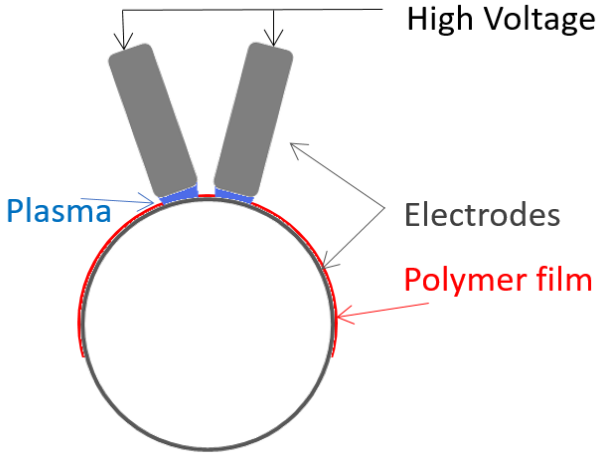

Figure 1. Schematic of the atmospheric pressure-plasma enhanced chemical vapor deposition (AP-PECVD) experimental setup: a uniform gas flow is injected between the two 30 cm long plasma zones. The polymer film is shown in red.

2.2 Input matrix

2.2.1 Parameters measured from the plasma

The input matrix was built from the plasma process experimental parameters and plasma properties, as determined from spectroscopic measurements because these variables are known to have a significant impact on the surface chemistry of plasma coated materials.[22]

2.2.2 Structure of the matrix

Figure 2 shows one set of the 16 different experimental conditions used to build up the input matrix. For each model, two sets of experiments were done for the training step, while one set of data was collected to test the model. The nitrogen gas flow, % of gaseous precursor, duty cycle, frequency and voltage amplitude are the parameters that were set up before the experiments. The power density, atomic nitrogen vibrational temperature (T_{vib}), FTIR emission and energy parameters were measured during the experiments according to the protocols described below.

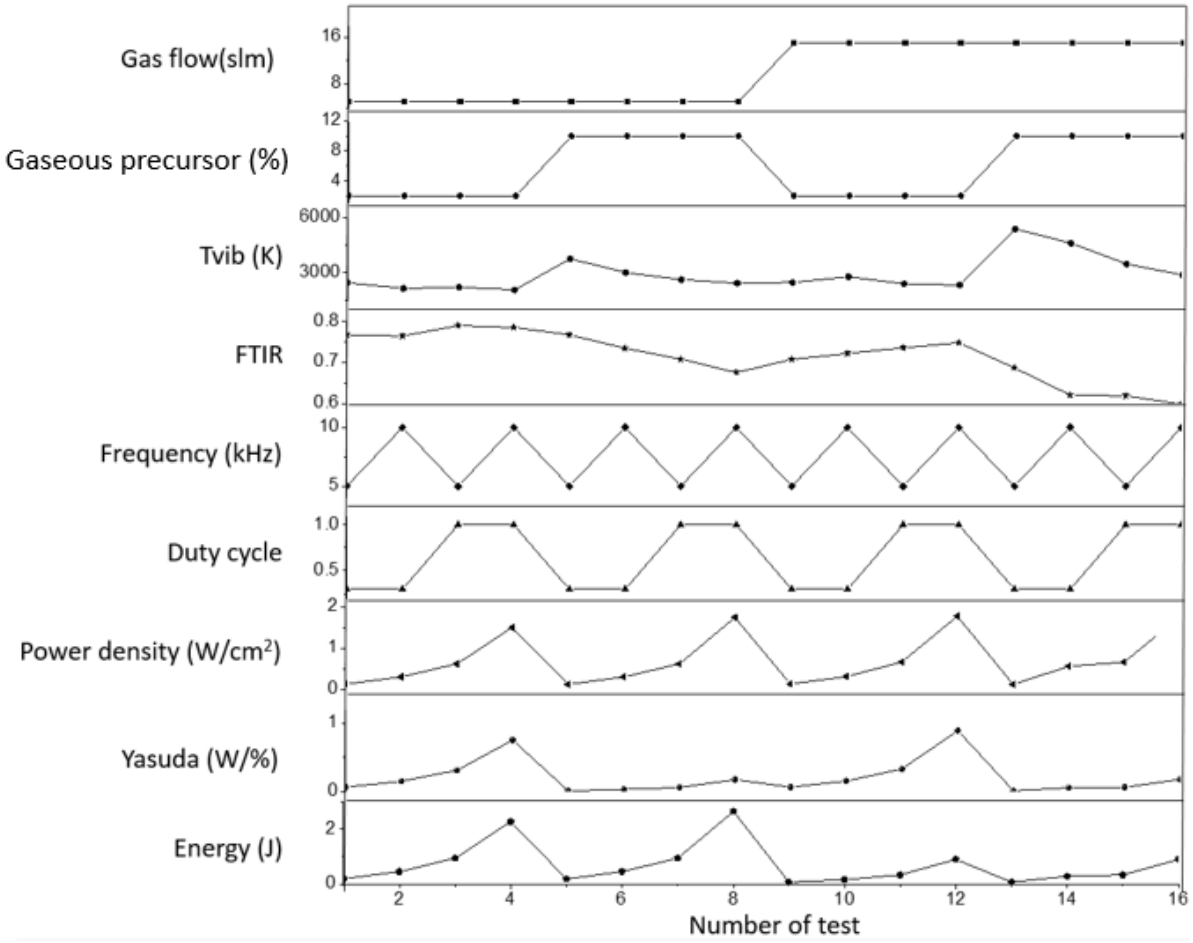

Figure 2. Example of one data set built using 16 different experimental conditions.

2.3 Plasma properties

Three methods were used to characterize the plasma. On one hand, the plasma power density, the energy "seen" by the precursor molecules, and power/amount of precursor (see below) in the plasma were calculated from the values of applied voltage, discharge current, gas flow, and precursor concentration measurements. On the other hand, infrared emission spectroscopy measurements were performed to probe the relative amount of unsaturated and saturated hydrocarbon-containing species in the plasma. Finally, UV-Vis emission spectroscopy was also used to determine the vibrational temperature of N_2 from the second positive system of nitrogen.[23-24]

2.3.1 Voltage and current measurements

In the case of a dielectric discharge, the current and applied voltage on the gas are not directly measurable because the capacitive current due to the dielectric is added to the discharge current. Therefore, the measured voltage is the sum of voltages applied to the gas and the dielectric. However, for a given period of time (t), the following equation enables calculating the mean power (P) of the discharge through the measurement of the total current (I_{mes}) and applied voltage (V_a):

$$P = \frac{1}{t}\int V_a . I_{mes} . dt \quad (1)$$

By using this equation, the integration of the capacitive power over the period is equal to zero. Therefore, only the power of the discharge is calculated.

The current probe used was a Pearson Electronics (Palo Alto, CA, USA) TMetrix 4100 with a ratio of 1 Volt/Amps. The high voltage was measured by a Tektronix probe (P6015A) which divided the signal by 1000. Both signals were read on a Tektronix DPO 2024A scope connected to a computer through a USB port. This setup made possible to perform real-time measurements and processing of current and voltage data. The scope signal was then transmitted to a computer and treated through a LabVIEW-based software (National Instruments Corp. Austin, TX, USA).

Using the electrical measurements, other parameters that characterize the chemical reaction in the plasma can be calculated. First, the energy "seen" by the gas during the plasma is characteristic of the number of precursor molecules dissociated in the plasma. The energy (E) was calculated by making the product of the residence time of the gas in the plasma and the power density (P):

$$E = P \cdot (gas\ residence\ time) \quad (2)$$

The second important parameter is the Yasuda's parameter that characterizes the "strength" of dissociation applied by the plasma on the gaseous precursor. Therefore, the Yasuda's parameter (Y) represents the power that is available to break down a given amount of precursor molecules.

$$Y = P / \%\ of\ gas\ precursor \quad (3)$$

2.3.2 FTIR emission spectroscopy

The measurements were done using an ABB FTLA 2000 spectrometer from ABB Analytical Measurements (Quebec City, Canada) which was located in front of the plasma, meaning that the optical direction was perpendicular to the gas flow and that the spectra were recorded according to the plasma long axis. One hundred scans (roughly corresponding to an acquisition time of 2 min) were routinely co-added with a liquid nitrogen-cooled MCT detector and Fourier transformed to yield a spectral resolution of 2 cm^{-1}. Contrary to low-pressure plasmas, which exhibit a large discharge volume, atmospheric pressure plasmas are confined to some millimeters corresponding to the gap between the electrodes. Accordingly, only little light is available to perform emission spectroscopy measurements at atmospheric pressure, therefore limiting the amount of information that could be obtained. Actually, the only useful signal was detected in the 2500-4000 cm^{-1} spectral region, where a large water emission feature is overlapped with two peaks assigned to unsaturated (left to 3000 cm^{-1}) and saturated (right to 3000 cm^{-1}) hydrocarbon-containing species (Figure 3).[25-26]

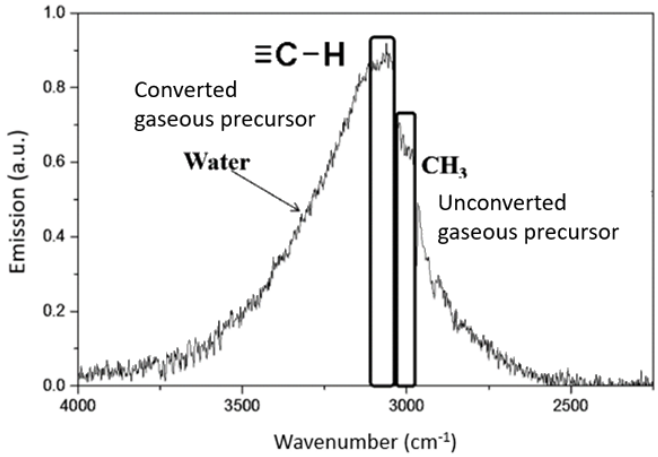

Figure 3. Infrared emission spectra of a plasma made in a nitrogen/gaseous precursor environment showing the water emission band overlapped with unsaturated and saturated carbon containing specie features.

Consequently, the h_{3050}/h_{2950} peak height intensity ratio can be used as a probe to monitor the transformation of the gaseous precursor in the plasma environment because this molecule contains aliphatic carbon atoms, potentially giving rise to the 2950 cm^{-1} band but is devoid of unsaturated carbon bonds. In this context, the 3050 cm^{-1} feature is most likely due to a partial conversion of the gaseous precursor into molecular species that contain unsaturated carbon bonds.

2.3.3 UV-Vis optical emission spectroscopy

UV-Vis spectroscopy was also used to get information about the energy of some of the excited species contained in the plasma environment. An HR4000 CG spectrometer from Ocean Optics (Dundin, FL, USA) was used to make the measurements by averaging 10 spectra acquired during 200 ms. The UV-Vis spectrometer was placed in front of the plasma perpendicularly to the gas flow as previously described for the FTIR emission measurements. Figure 4a shows the overall UV-Vis spectrum of a plasma made in a mixture of nitrogen and the gaseous precursor whereas Figure 4b focuses on the Δv = -2 transition of the nitrogen second positive system. The decrease in intensity observed for these bands is due to the fact that the vibrational levels from which these transitions occur, and to which they end up, are not equally populated. In fact, for a given electronic state, the relative distribution of the vibrational levels is described through a Boltzmann distribution. Therefore, the electronic transition between two vibrational states can be used to calculate the vibrational temperature of nitrogen in the plasma according to the following equations:

$$I_{vv'} = C(\lambda_{vv'})hV_{vv'}A_{vv'}\left[N(v=0)\right]e^{-(E_v-E_0)/kT_{vib}} \tag{4}$$

and

$$\ln\left(\frac{I_{vv'}}{V_{vv'}A_{vv'}}\right) = const - \frac{E_v - E_0}{kT_{vib}} \tag{5}$$

where
$I_{vv'}$: Intensity of a single vibrational band
$V_{vv'}$: Transition frequency

$A_{vv'}$: Spontaneous transition probability
E_v: Energy of the v level
E_0: Energy of the ground state
k: Planck's constant
T_{vib}: Vibrational temperature

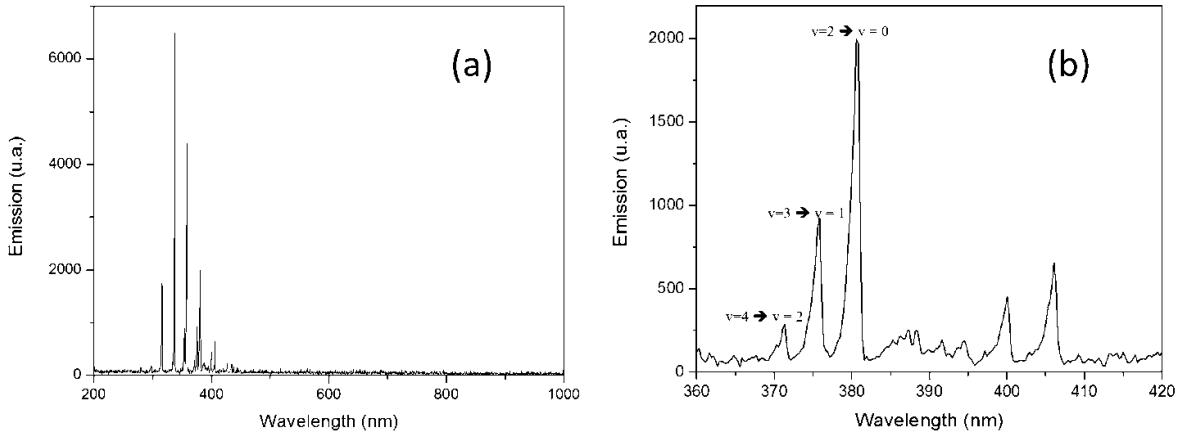

Figure 4. UV-Vis emission Spectrum of a plasma made with a mixture of nitrogen and gaseous precursor. (a) Overall spectrum; (b) spectral region used to make rotational temperature calculations.

2.4 Output matrix composition

Concomitantly with plasma characterization, surface analyses were performed to correlate plasma characteristics with the resulting coating chemistries.

2.4.1 XPS

The surface chemistry of the plasma-deposited coatings was investigated by recording low-resolution x-ray photoelectron spectra using a PHI 5600-ci apparatus (Physical Electronics USA, Chanhassen, MN, USA) equipped with a standard aluminum X-Ray source at 300 W (1486,6 eV). A low energy electron neutralizer was used for charge compensation. The detection was performed at 45° with respect to the surface normal with a pass energy of 187.5 eV, giving rise to a spectral resolution of 1.4 eV. Relative surface concentrations in terms of carbon, oxygen, fluorine and nitrogen were determined using the sensitivity factors provided in the manufacturer's software (Multipak v9.3) after performing a baseline correction with a Shirley type function.

2.4.2 Surface Energy

The surface energy was calculated using the Wu's model, which requires the measurement of the static contact angle with two different liquids.[27] This model is recommended for the determination of polymer surface energy. Accordingly, surface energy was calculated from the contact angle values measured with water and dimethylformamide on the plasma treated fluoropolymer surfaces. The contact angles were measured using a VCA optima XE from AST Products, Inc. (Billerica, MA, USA), after stabilization of the liquid droplets (0.3 ml). As an indication, depending on the experimental plasma parameters investigated, water contact angles on PTFE varied from 120° for untreated PTFE to values as low as 10° while that of dimethylformamide ranged from 5° to 42°, therefore leading to surface energy values between 28mJ/m^2 to 72mJ/m^2.

2.4.3 ATR-FTIR

The ATR-FTIR (Attenuated Total Reflectance FTIR) spectra of the plasma-deposited coatings on the different fluoropolymers were recorded with an Agilent 660 IR spectrometer (Santa Clara, CA, USA) equipped with a DTGS detector. Sixteen scans were routinely co-added and Fourier transformed to yield a spectral resolution of 4 cm^{-1}. The spectra were used to monitor the relative coating thickness of the plasma deposited layers on the various fluoropolymers. Figure 5 shows spectra of ETFE before and after 1 second of plasma treatment. Three new absorption bands can be observed on the treated films. The band observed between 3200 and 3600 cm^{-1} is attributed to OH stretching.[28] The feature appearing near 2200 cm^{-1} was seen only on plasma-treated ETFE films and was not observed for the two other plasma-treated fluorinated polymers investigated in this study. This bands is most like due to C≡N and/or C≡C moieties.[29] Finally, the third band observed after plasma treatment is a large feature arising between 1500 and 1800 cm^{-1}, and is most likely due to the overlap of infrared peaks assigned to N=O stretching, C=O stretching, and N-H bending.[30,31] Because, on one hand, the absorbance of this new infrared feature was fairly intense and, on the other and, this peak was quite well isolated from the fluorinated polymers spectra (Figure 5), its integrated intensity was normalised to that of peaks characteristic of each polymer (1452 cm^{-1} for ETFE, 1205 cm^{-1} for FEP, and the integrated area of the spectral region between 1000 and 1270 cm^{-1} for PTFE). These ratios were used as a probe of the deposited layer thickness.

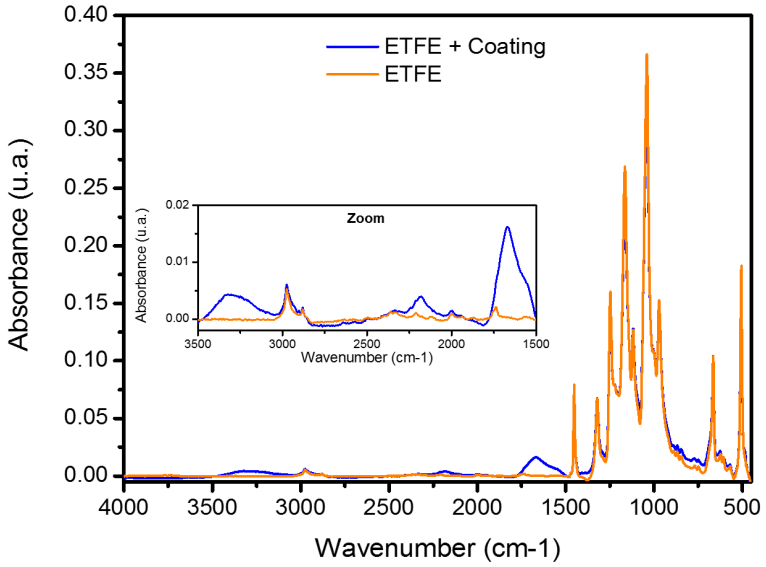

Figure 5. ATR-FTIR spectra of treated (blue) and untreated ETFE (orange)

2.5 PLSR model

Traditionally, multiple linear regression (MLR) is used to model a response matrix (Y) using a predictive (X) matrix, as long as only a few X-variables are available and are fairly uncorrelated.[32] However, as plasma process conditions and emission spectroscopy results (the X-variables) are correlated, partial least square regression (PLSR) approaches should be definitely privileged. In fact, the prediction by PLSR is achieved by extracting, from X, a set of orthogonal components defined as linear combinations of the original X-variables. These so-called latent variables (or principal components) relate the two blocks of variables, namely X and Y, in a way that maximizes the covariance between them.[20] In other words, these linear combinations are the most predictive of Y.

In order to elaborate an accurate model, the number of principal components to be considered has to be carefully chosen. These principal components may be seen as orthogonal vectors arising from the projection of two data spaces with large number of correlated dimensions into a second

data space with much smaller number of independent dimensions. Basically, this number of principal components is selected to minimize the root mean Predictive Residual Sum of Squares (PRESS). PRESS is the gap between the model prediction values and the actual measured values. In addition, the number of principal components is also selected to maximize R^2 and Q^2. R^2 is the percentage of X data explained by the model while Q^2 is the cross-validated R^2, which is the amount of Y data predicted by the X scores. In other words, R^2's give an upper bound of how well the model explains the data and predicts new observations, and the Q^2 's give a lower bound for the same things. [32]

The objective of PLSR is actually to model the relationships between the X (N × K) and Y (N × M) matrices as well as within each data block, through the following bilinear decomposition.[33] In the present study, a 2^4 full factorial design was used with N=16 (number of experiments), K=9 (number of experimental parameters in the input matrix), and M=7 (number of surface characterization parameters inserted in the output matrix):

$$X= TP'+E \tag{6}$$

$$Y= TQ'+F \tag{7}$$

$$T= XW^* \tag{8}$$

Where P (K × r) and Q (M × r) are the loading matrices for the X and Y spaces, respectively, and W* is the so-called weight matrix containing those linear combinations of X-variables that are the most predictive of Y. The results of calculating the linear combinations of the X-variables for each observation (i.e., row of X) are stored in the score matrix T. The model residuals for the X and Y data are collected in the E and F matrices, respectively.

For prediction purposes, Equations 6-8 can be rewritten in a form similar to that of a multiple regression model:

$$Y= XW^* Q'+F = XB+F \tag{9}$$

The PLS-regression coefficients B, are represented as follows:

$$B= W^*Q' \tag{10}$$

PLSR modelling also makes it possible to quantify the importance of each variable on the projection model, thus enabling the identification of the relative importance of the input variables in a given process, such as a plasma surface modification. This is achieved by calculating the variable importance on the projection (VIP):[34]

$$VIP_k = \sqrt{\frac{K\sum_{a=1}^{r}\left(\left(\frac{w_{ak}}{\|w_a\|}\right)^2 (q_a^2 t_a' t_a)\right)}{\sum_{a=1}^{r}(q_a^2 t_a' t_a)}} \tag{11}$$

Where K is the total number of variables, w_{ak} is the weight of the k^{th} variable for principal component a, r is the number of the principal components, and w_a, t_a and q_a are the a^{th} column vectors of W, T and Q, respectively.

According to Eriksson et al., the variables with a VIP greater than 1 have more influence in the model because the average of the squared VIPs is equal to 1.[33] The variables with a VIP between 0.8 and 1.0 have moderate influence, while a VIP of less than 0.8 are less important variables. For more details on PLSR, the reader is referred to Wold et al.[32]

The correlation between the predictive matrix X (the plasma parameters) and the response matrix Y (the surface properties) was determined by applying a PLSR analysis using commercial softwares (either ProSensus or JMP12). Both softwares gave the same results and led to identical conclusions.

The process conditions were adjusted prior to each experiment while the plasma parameters were measured using UV-visible, IR emission spectra and electrical measurements. Plasma frequencies of 5 and 10 kHz were investigated with duty cycles ($T_{on}/(T_{on}+T_{off})$) of 0.3 and 1 for a total cycle of 5 ms. Gas flows of 5 and 10 slm were used with 2 and 10 % of gaseous precursor for a total of 16 experimental conditions. Considering these experimental parameters and those resulting from calculation (Figure 2), this led to a X matrix of (16x9). The surface characteristic parameters used to construct the Y matrix consisted of atomic surface concentration data as determined by XPS (%C, %F, %O and %N), surface energy, and ATR-FTIR measurements. In addition, the intensity of the infrared feature located near 2200 cm-1 was measured for ETFE, therefore leading to a Y matrix of (16 x 6) for PTFE and TFE and of (16 x 7) for ETFE. As three replicates were made for each process condition, two set of data were used to build up the training set of matrices, while one data set of matrices was used to validate the model.

3 RESULTS AND DISCUSSION

Figure 6 shows the PRESS and values of R^2 and Q^2 as a function of the number of components used to build up the PLS model for all polymers investigated. Figure 6a shows that the best models for FEP and PTFE are obtained with 7 components, with root mean PRESS decreasing down to 0.5 and 0.6, respectively. On the other hand, 9 components are necessary to decrease the root mean PRESS to 0.6 for ETFE. For such numbers of principal components, the R^2 values are above 93 %, while Q^2 reaches 80% , 75%, and 70 % for FEP, PTFE, and ETFE, respectively (Figure 6b), therefore meaning that more than 90% of the training data are within one standard deviation from the actual experimental values while 70 to 80% of the test data are accurately predicted within one standard deviation.

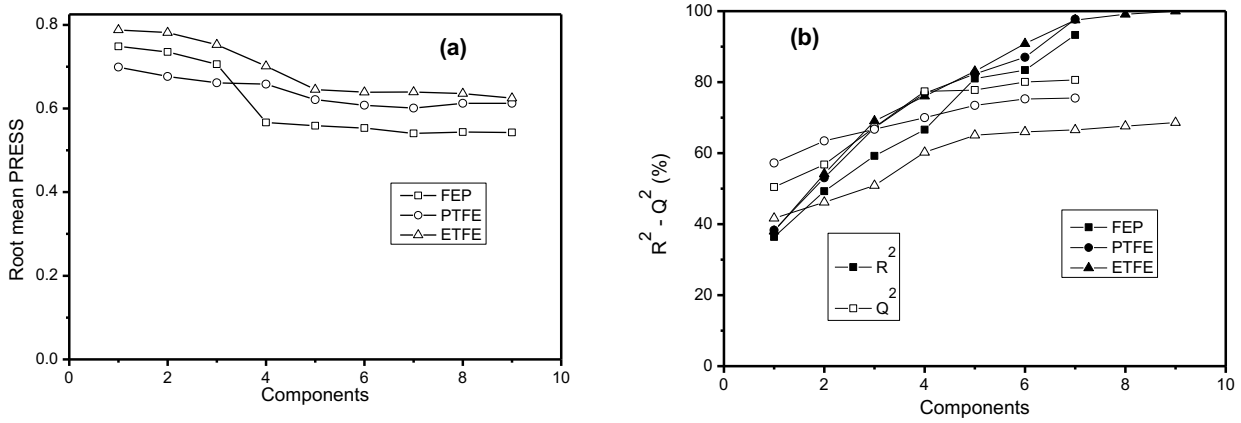

Figure 6. (a) Root mean PRESS and (b) R^2 and Q^2 as a function of the number of components of the models for the three polymers

This is confirmed in Figure 7, where the Q^2 values are given for each of the surface characterization parameters that were investigated for all three polymers. Figure 7 shows that for FEP, most parameters of interest may be predicted with a fairly high level of confidence (higher than 80%), with the exception of the oxygen surface concentration. A similar situation is observed with

PTFE with most of the Q^2 values being higher than 75%. Finally, the ETFE model is somewhat less satisfactory, especially in terms of this treated polymer surface chemistry as determined by XPS.

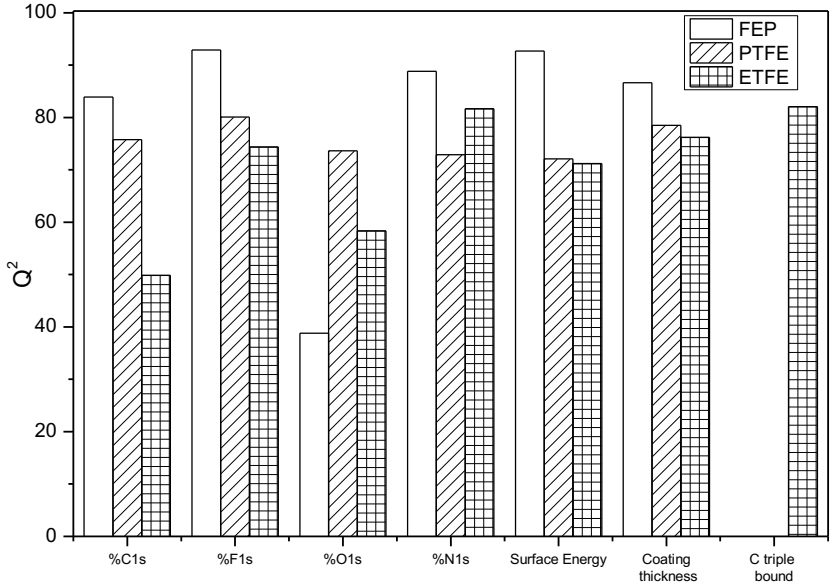

Figure 7. Q^2 for each output variable for the FEP, PTFE and ETFE models

The difference of model quality can be explained by a difference in the complexity of the chemical composition of the polymer. Indeed, FEP and PTFE are made only of carbon and fluorine atoms while the ETFE also contains hydrogen in addition to carbon and fluorine. As discussed by Nassef et al., [35] the initial reactions occurring on the surface of ETFE films exposed to electron irradiation involve scission of C-F, C-H and C-C bonds, therefore leading to the formation of macroradicals, which may undergo competitive reactions such as (1) peroxidation by reaction with atmospheric oxygen leading to formation of hydroperoxides after hydrogen abstraction from the neighbouring ethylene molecules; (2) dehydrofluorination after C–C scission to form unsaturated structures; (3) dehydrofluorination and the subsequent formation of crosslinked structures by reaction with adjacent macromolecular radicals.[35] Accordingly, the complexity of chemical reaction kinetics on the surface of ETFE is probably at the origin of the less satisfactory prediction of PLS regression for this polymer. A more accurate prediction would probably need to integrate more than the 16 sets of experiments to build up the Y matrix. As the behaviour of the nitrogen and fluorine surface concentration is fairly well predicted, it is likely that the incorporation of oxygen and carbon from the precursor that is injected in the plasma highly depends on the polymer chemical structure.

Examples of the prediction provided by the PLS model are presented in Figure 8. Figure 8a displays the actual measured nitrogen surface concentration as a function of the nitrogen surface concentration predicted by the model for FEP. As may be seen, the nitrogen surface concentration is fairly well predicted by the model, with the exception of the highest surface concentration values (>22-23%), which explains why R^2 is slightly different from 1. Also presented in this figure (Figure 8b) is the measured surface energy as a function of the surface energy predicted by the model. In this case, the prediction is rather good with R^2=0.963.

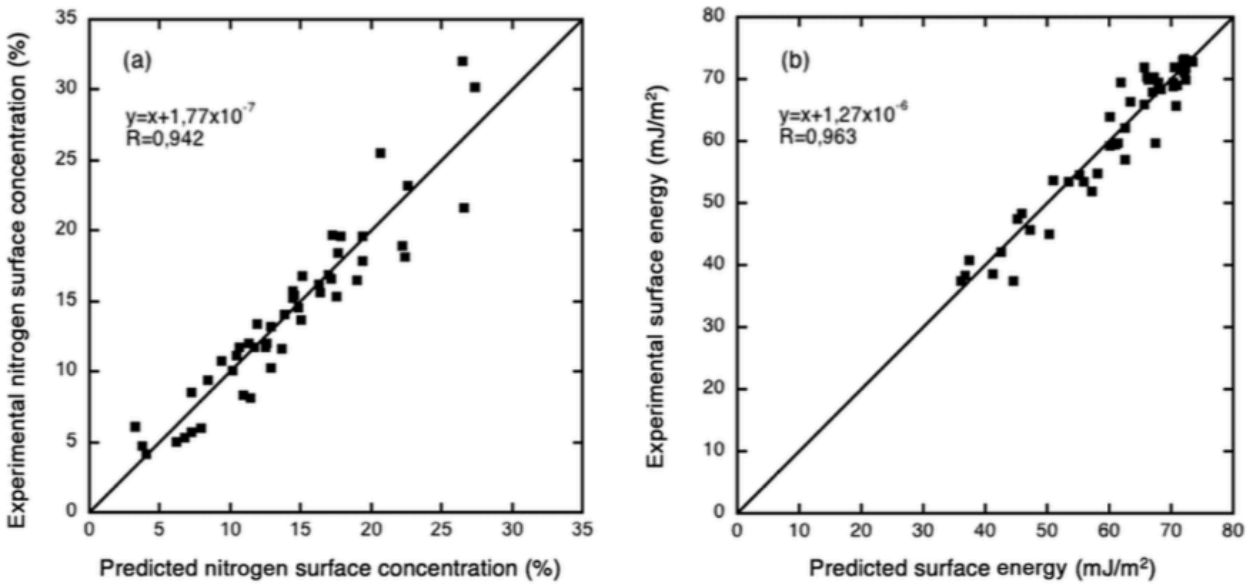

Figure 8. (a) Observed relative nitrogen surface concentration as a function of the predicted relative nitrogen surface concentration and (b) observed surface energy as a function of the predicted surface energy for FEP.

The PLS model also enables calculating the variable importance on the projection (VIP) or, in other words, the importance of each of the plasma experimental parameters/spectroscopic characteristics on the physicochemical properties of the plasma treated polymer surface, as shown in Figure 9. It is generally well accepted that a VIP value above 0.8 is representative of a parameter that impacts the surface physicochemical properties.[32] As shown in Figure 9, the electrical parameters are critical to control the process. The most important input parameters are power density and duty cycle. In addition, the Yasuda's parameter (which is characteristic of the organic molecules decomposition scheme) and the energy (which is related to the amount of dissociated molecules) are also very important to control the polymer surface properties.

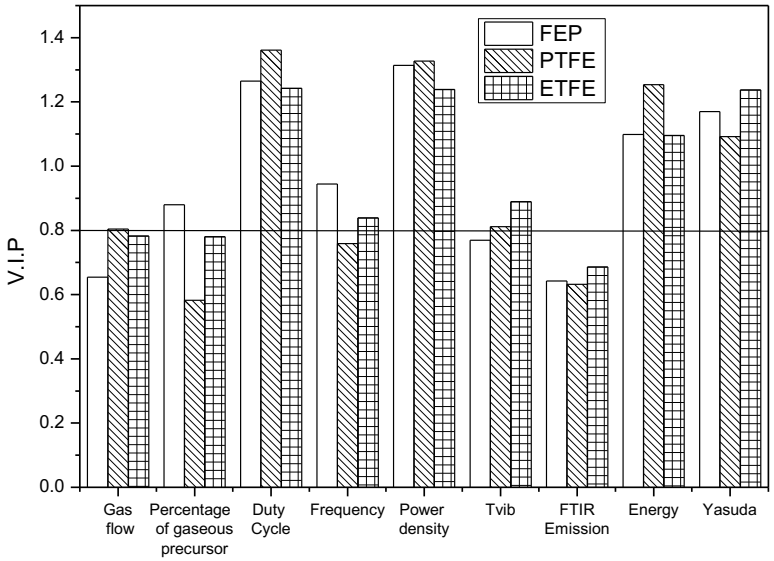

Figure 9. V.I.P. for treated FEP, PTFE and FEP models

As shown in Figure 10, the biplot enables to evidence correlations between parameters (either input or output). Essentially, a correlation exists for parameters located on the same side of the origin of the x-axis of the biplot graph. For example, “evident” relationships are found for all three polymers, such as the fluorine surface concentration that is anti-correlated with the nitrogen surface concentration, therefore providing credibility to the models. However, the biplot also allows to evidence that the coating thickness is generally well correlated with parameters depending on the electrical characteristics of the discharge such as the electrical power, frequency, duty cycle, energy, and Yasuda’s parameter. For example, a clear correlation exists between the power provided to the discharge and the coating thickness for all three investigated polymers.

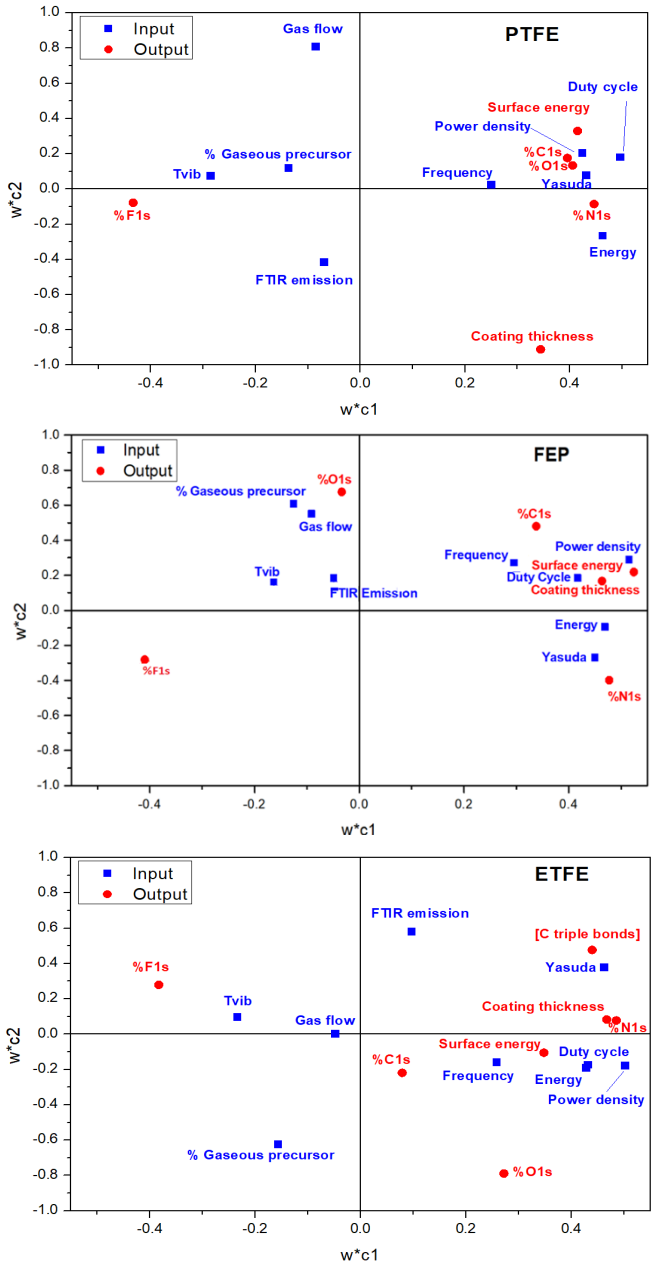

Figure 10. Biplots for FEP, PTFE and FEP models. w*c1 and w*c2 are the first and second principal components, respectively.

From the data shown in Figure 10, general trends can be deduced on the relationship between the plasma operation parameters and the coating properties. First, the coating thickness, and hence, the fluorine surface concentration, strongly depend on plasma experimental parameters related to the power injected in the discharge. Indeed, from the biplots, the coating thickness is clearly correlated with plasma operation parameters such as frequency, energy, power density, Yasuda parameter, and duty cycles, which are all, to some extent, related to the energy provided to the precursor molecules. Of course, this coating thickness increase is accompanied with a decrease of the F1s XPS signal, as evidenced in the biplots by the anticorrelation of %F and all parameters related to the power injected in the discharge. Such a behavior (e.g. coating thickness increase with the amount of power provided to the discharge) is in agreement with previously published data by Brunet et al.[36] In this context, it is not surprising to observe that the biplots indicate that both coating thickness and surface energy are correlated, as the progressive coverage of the highly hydrophobic (low surface energy) fluorinated surfaces by the plasma deposited coatings is likely to increase the overall surface energy.

Therefore, the biplots presented in Figure 10 bring essential information about the treatment process. Indeed, if the aim of this treatment is to increase the surface energy, one should definitely try to increase the coating thickness, which is, in turn, correlated with the parameters depending on the plasma electrical characteristics. Other non-trivial relationships may also be deduced. For instance, the surface coating thickness increases by decreasing the amount of organic precursor or the gas flow in the discharge. This counter-intuitive result possibly evidences the importance of integrating the Yasuda's parameter and energy values in the model. In other words, putting too much precursor in the discharge leads to less power provided to each precursor molecule, therefore affecting the precursor breakdown process that is necessary to build up the coating.

PLSR therefore offers several advantages to study plasma processes. On one hand, contrary to a simple array of scatter plots, PLSR enables to determine correlations between parameters while considerably minimizing the amount of experiments to be performed. On the other hand, as opposed to Multiple Regression Linear Analysis, for which calculations of interactions between parameters are made for a single response variable, PLSR rather leads to information such as score and loading plots when several response variables come into play. Finally, PLSR analysis can be performed even with strongly correlated x-variables.[31] This is the case for the present study where energy, power density, frequency, duty cycle, and Yasuda's parameter are all somewhat related to the overall energy provided to the gaseous precursor molecules.

At this point, one could question the influence of individual measurement uncertainties on the overall PLSR model. Wolthuis et al.[37] estimated the influence of experimental errors on the prediction error of PLS calibration models based on Raman spectra and concluded that it is very difficult to assess the propagation of the different errors in the total prediction error. It was therefore suggested to use a systematic approach, based on simulation and measurements of a simple two-component system to identify and prioritize possible improvements in both hardware and experimental protocols. This leads to a possible improvement of the accuracy and robustness of more complex multi-component models.

4 CONCLUSION

This study demonstrates the potential of PLSR to correlate the characteristics of DBD atmospheric plasma deposited coatings on fluoropolymers with the plasma process conditions. On one hand, a plasma made in a mixture of nitrogen and a gaseous precursor was characterized through electrical and emission spectroscopy measurements. On the other hand, the physicochemical properties of the plasma deposited coatings on fluorinated polymers were ascertained through XPS, FTIR, and contact angle measurements. The PLSR correlation performed between these two sets of data clearly demonstrated the importance of the plasma electrical parameters on the resulting properties of the coating. Once this correlation is obtained, an

appropriate selection of the plasma electrical input parameters allows determining the coatings characteristics without having to perform time-consuming post plasma analyses of the layer. That said, the selection of the parameters to be investigated in terms of plasma characterization (input matrix) was based on their expected importance on plasma-deposited coating chemistries deduced from the relevant literature on the field, but also on the characterization techniques available in our laboratory. This means that a similar mathematical approach using other plasma characterization techniques is likely to provide other interesting information to control plasma processes.

ACKNOWLEDGEMENTS

The authors would like to express their gratitude to Dr Nicolas Naudé from LAPLACE-CNRS, Université Paul-Sabatier in Toulouse, France, for providing the Lab-VIEW based software used to record the electrical signals originating from the plasma discharge, and Alex Gélinas for his technical assistance. They also thank Saint-Gobain, Northboro, MA, for financial support. The collaboration of Nicolas Drolet and Camila Garces from Saint-Gobain Performance Plastics (Northboro, MA) was deeply appreciated.

REFERENCES

(1) Teng, H. Overview of the Development of the Fluoropolymer Industry Appl. Sci. 2012, 2, 496.
(2) Magdzinski, L. Select the Right Fluoropolymer for your Plant Chem. Eng. Prog. 2000, 96, 21.
(3) Kavan, L. Electrochemical Carbon Chem. Rev. 1997, 8, 3061.
(4) Kavan, L.; Dousek, F.P; Doblhofer, K. Electrochemical Reductive Caronization of Polymers Derived from Hexafluoropropene J. Fluorine Chem. 1991, 55, 37.
(5) Sarra-Bournet, C.; Ayotte, G.; Turgeon, S.; Massines, F.; Laroche, G. Effects of Chemical Composition and the Addition of H2 and N2 Atmospheric Pressure Dielectric Barrier Discharge on Polymer Surface Functionalization. Langmuir, 2009, 25, 9432.
(6) Mandracci, P.; Ricciardi C. Silicon–Carbon–Oxynitrides Grown by Plasma-Enhanced Chemical Vapor Deposition Technique. Thin Solid Films, 2007, 515, 7639.
(7) Yang, P.; Huang, N.; Leng, Y.; Chen, J.; Wang, J.; Sun, H.; Wan, G.; Zhao, A. Wettability and Bloodcompatibility of a-C:N:H Films Deposited by PIII-D. Surf. Coat. Technol. 2010, 204, 3039.
(8) Vallade, J.; Bazinette, R.; Gaudy, L.; Massines, F. Effect of Glow DBD Modulation on Gas and Thin Film Chemical Composition: Case of Ar/SiH4/NH3 Mixture. J. Phys. D Appl. Phys. 2014, 47, 224006.
(9) Michel, B.; Giza, M.; Krumrey, M.; Eichler, M.; Grundmeier, G.; Klages, C.-P. Effects of Dielectric Barrier Discharges on Silicon Surfaces: Surface Roughness, Cleaning, and Oxidation. J. Appl. Phys. 2009, 105, 073302.
(10) Asandulesa, M.; Topala, I.; Dumitrascu, N. Effects of Plasma Treatments on the Surface of Wood Samples. Holzforschung 2010, 64, 223.
(11) Taghvaei, H.; Kheirollahivash, M.; Ghasemi, M.; Rostami, P.; M. Rahimpour, R. Noncatalytic upgrading of anisole in an atmospheric DBD Plasma Reactor: Effect of Carrier Gas Type, Voltage, and Frequency. Energ. Fuel. 2014, 28, 2535.
(12) Swatowska, B.; Kluska, S.; Jurzecka-Szymacha, M.; Stapinski, T.; Tkacz-Smiech, K. The Chemical Composition and Band Gap of Amorphous Si:C:N:H Layers. Appl. Surf. Sci. 2016, 371, 91.
(13) Pankaj, S.; Bueno-Ferrer, C.; Misra, N.N.; Neill, L.O.; Tiwari, B.K.; Bourke, P.; Cullen, P.J. Characterization of Dielectric Barrier Discharge Atmospheric Air Cold Plasma Treated Gelatin Films. Food Packaging and Shelf Life, 2015, 6, 61.
(14) Sophonvachiraporn, P.; Rujiravanit, R.; Sreethawong, T.; Tokura, S.; Chavadej, S. Surface Characterization and Antimicrobial Activity of Chitosan-Deposited DBD Plasma-Modified Woven PET Surface. Plasma Chem. Plasma Process. 2011, 31, 233.

(15) Borra J.P.; Valt A.; Arefi-Khonsari, F.; Tatoulian, M. Atmospheric Pressure Deposition of Thin Functional Coatings: Polymer Surface Patterning by DBD and Post-Discharge Polymerization of Liquid Vinyl Monomer from Surface Radicals. Plasma Process. Polym. 2012, 9, 1104.

(16) Kostov, K.G. ; dos Santos, A.L.R. ; Nascente, P.A.P. ; Katama, M.E. ; Mota, P. ; M.A. Algatti, Surface Modification of Siloxane Containing Polyurethane Polymer by Dielectric Barrier Discharge at Atmospheric Pressure. J. Appl. Polym. Sci. 2012, 125, 4121.

(17) Paisoonsin, S.; Pornsunthorntawee, O.; Rujiravanit, R. Preparation and Characterization of ZnO-Deposited DBD Plasma-Treated PP Packaging Film with Antibacterial Activities. Appl. Surf. Sci. 2013, 273, 824.

(18) Favia, P.; Stendardo, M.; d'Agostino R. Selective Grafting of Amine Groups on Polyethylene by Means of NH3−H2 RF Glow Discharges. Plasmas Polym. 1996, 1, 91.

(19) Wang, M.; Chang, Y.; and Poncin-Epaillard, F.; Effects of the Addition of Hydrogen in the Nitrogen Cold Plasma: The Surface Modification of Polystyrene. Langmuir, 2003, 19, 8325.

(20) Höskuldsson A. PLS Regression Methods. J. Chemometr. 1988, 2, 211.

(21) Mavadat, M.; Ghasemzadeh, M.; Turgeon, S.; Duchesne, C.; Laroche, G. Correlation between the Plasma Characteristics and the Surface Chemistry of Plasma-Treated Polymers through Partial Least-Squares Analysis Langmuir, 2013, 29, 15859.

(22) Massines, F.; Sarra-Bournet, C.; Fanelli, F.; Naudé, N.; Gherardi, N. Atmospheric Pressure Low Temperature Direct Plasma Technology: Status and Challenges for Thin Film Deposition. Plasma Process. Polym. 2012, 9, 1041.

(23) Q.Y. Zhang, D.Q. Shi, W. Xu, C.Y. Miao, C.Y. Ma, C.S. Ren, C. Zhang, and Z. Yi, Determination of Vibrational and Rotational Temperatures in Highly Constricted Nitrogen Plasmas by Fitting the Second Positive System of N2 Molecules. AIP Adv. 2015, 5, 057158.

(24) Isola, L.; López, M.; Gómez, B.J. Study of the Excitation Mechanisms of the Second Positive System in the Negative Glow of a N2–Ar Discharge. J. Phys. D Appl. Phys. 2011, 44, 375204.

(25) Leclerc, H.; Vimont, A.; Lavalley, J.-C.; Daturi, M.; Wiersum,A.D.; Llwellyn, P.L.; Horcajada, P.; Ferey, G.; Serre, C. Infrared Study of the Influence of Reducible Iron(III) Metal Sites on the Adsorption of CO, CO2, Propane, Propene and Propyne in the Mesoporous Metal-organic Framework MIL-100. Phys. Chem. Chem. Phys. 2011, 13, 11748.

(26) Es-sebbar, Et.; Jolly, A.; Benilan, Y.; A. Farooq, Quantitative Mid-infrared Spectra of Allene and Propyne from Room to High Temperatures. J. Mol. Spectrosc. 2014, 305, 10.

(27) Wu, S. Calculation of Interfacial Tension in Polymer Systems. J. Polymer Sci. 1971, 34, 19.

(28) L. Kellner, P. R. Soc. The near-infrared absorption spectrum of heavy water
London Ser A, 1937, 159, 410.

(29) Lanzisera, D.V.; Andrews, L. Reactions of Laser-Ablated Beryllium Atoms with Hydrogen Cyanide in Excess Argon. FTIR Spectra and Quantum Chemical Calculations on BeCN, BeNC, HBeCN, and HBeNC. JACS, 1997, 119, 6392.

(30) Foerstendorf, H.; Benda, C.; Gärtner, W.; Storf, M.; Scheer, H.; and Siebert, F. FTIR Studies of Phytochrome Photoreactions Reveal the C=O Bands of the Chromophore: Consequences for its Protonation States, Conformation, and Protein Interaction. Biochemistry, 2001, 40, 14952.

(31) Sim, S.F.; and Ting, W. An Automated Approach for Analysis of Fourier Transform Infrared (FTIR) Spectra of Edible Oils. Talanta, 2012, 88, 537-543.

(32) Wold, S.M.; Sjöström, M.; Eriksson, L. PLS-Regression: a Basic Tool of Chemometrics. Chemometr. Intell. Lab. 2001, 58, 109.

(33) Multi- and Megavariate Data Analysis, Basic Principles and Applications, L. Eriksson, E. Johansson, N . Kettaneh-Wold N, and S. Wold, Eds., Umetrics Academy, 3rd edition, 2013.

(34) Gaudet, S.; Janes, K.A.; Albeck, J.G.; Pace, E.A.; Lauffenburger, D.A.; and Sorger, P.K. A Compendium of Signals and Responses Triggered by Prodeath and Prosurvival Cytokines. Mol. Cell. Proteomics, 2005, 4, 1569.

(35) Nasef, M.M.; Saidi, H.; Dahlan, K.Z.M.; Electron beam irradiation effects on ethylene-tetrafluoroethylene copolymer films. Radiat. Phys. Chem. 2003, 68, 875.

(36) Brunet, P. ; Rincón, R.; Margot, J.; Massines, F.; Chaker, M. Deposition of Homogeneous Carbon-TiO2 composites by Atmospheric Pressure DBD, Plasma Process. Polym. 2017, 14, c1700049.

(37) Wolthuis, R.; Tjiang, G.C.H.; Puppels G.J.; Bakker Schut, T.C. Estimating the Influence of Experimental Parameters on the Prediction Error of PLS Calibration Models based on Raman Spectra, J. Raman Spectrosc. 2006, 37, 447.